Analysis of Biaxially Stressed Bridge Deck Plates

Jönsson, Jeppe; Bondum, Tommi Højer

Published in:
Proceedings of Nordic Steel Construction Conference 2012

Publication date:
2012

Nordic Steel Construction Conference 2012
Hotel Bristol, Oslo, Norway
5-7 September 2012

ANALYSIS OF BIAXIALLY STRESSED BRIDGE DECK PLATES

Jeppe Jönsson, Tommi Højer Bondum

DTU Civil Engineering, Technical University of Denmark

Abstract: The ultimate state analysis of bridge deck plates at the intersection zone between main girders and transverse beams is complicated by biaxial membrane stresses, which may be in compression or tension in either direction depending on the bridge configuration and the specific location. This paper presents a detailed investigation of the ultimate capacity of simply supported plates subjected to biaxial loads. The full interaction domain of combinations of compressive and tensile loads has been investigated including a large number of imperfections. It was found that non-standard imperfection modes in parts of the interaction domain lead to more critical and lower ultimate capacity than critical buckling mode imperfections.

1 Introduction

In modern steel highway bridges it is becoming more common to separate the bridge girder into two girders which are joined at intervals by stiffening transverse beams as an important integral part of the bridge structure. The ultimate state analysis of bridge deck plates at the intersection zone between the main girders and the transverse beam includes biaxially membrane stresses which may be in compression or tension. The analysis and design of these zones are not well described in the codes and it is not clear whether or not the effective width approach can be generalized to enable full utilization of any post-buckling capacity.

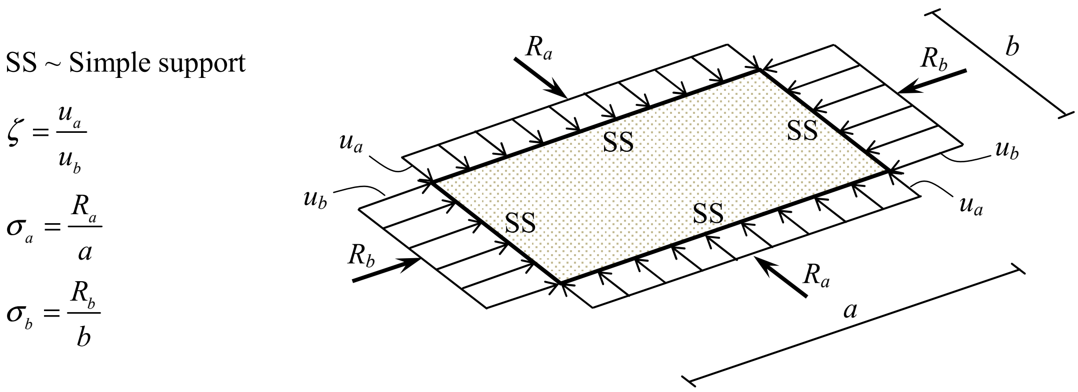

Fig. 1: Biaxially loaded plate with proportional uniform edge displacements

The presented investigations are based on advanced non-linear finite element analysis of rectangular simply supported plates with proportional uniform in plane edge displacements as shown in Fig. 1. The research includes detailed investigations of the behaviour of plates in the complete interaction domain with a main focus on the influence of the imperfection shape and magnitude. A large number of applied imperfection shapes, constituted by relevant buckling modes, are included in the investigation. The research is based on an imperfection magnitude according to the provisions in EN 1993-1-5 and a novel proposal for the short wave imperfection magnitude is given by the authors. Based on the obtained results conservative interaction curves and corresponding buckling reduction curves are established. The research includes investigations of various slendernesses and aspect ratios, however, we have chosen in this paper to illustrate our work using an aspect ratio of $\alpha = 4$ and a slender plate corresponding to a width to thickness ratio of *b/t*=125. However, interaction curves and buckling reduction curves for additional slenderness values are presented. Our calculation are based on a yield stress of $f_y = 350\text{MPa}$, Poisson ratio of $\nu = 0.3$, elastic modulus of $E = 2.1 \cdot 10^5\text{MPa}$ and a tangent hardening modulus of $E_h = 0.01E$. The plate is considered simply supported and the edges are assumed to remain straight. The loading of the plate is based on forced proportional biaxial edge displacements. The numerical research is based on the provisions in Annex C of EN 1993-1-5 [1] and performed using the finite element program ABAQUS [2]. The geometrical and material non-linear analysis is mainly based on imperfection modes prescribed in Annex C of EN 1993-1-5 as a fraction of the critical (first) buckling mode and on a bi-linear material description using the Von Mises type yield criterion extended to include linear hardening. However further investigations showed that these imperfections may not be conservative in the whole interaction domain.

In the typical analysis performed in the presented work we first carry out a linear buckling analysis (LBA) in order to obtain the relevant critical buckling loads and buckling mode shapes. Following this a geometrical and material nonlinear imperfect analysis (GMNIA) is carried out to determine the second order elastic-plastic ultimate capacity of the plates and for those susceptible to buckling the post-buckling capacity is determined. In the case of a snap through type behaviour (due to buckling mode transition) the highest peak capacity in the main loading direction is used. This is in contrast to the provisions used in shell buckling design, where asymmetric bifurcations prevent increased post buckling capacity, see Section 8.7 in EN 1993-1-6 [3].

Plates subjected to combined loads have been studied extensively during the previous decades. The majority of studies are theoretically based numerical research and only a limited number of experiments have been conducted. In the following a review on earlier work is performed in order to investigate the influence of the assumptions on which the present research is built. In the thesis of Braun [4] (Section 5.4.4) a numerical study of the influence of edge boundary conditions on the ultimate plate capacity is reported for plates with aspect ratios of $\alpha = 1$ and $\alpha = 3$. In this work Braun compares the interaction curves of plates with respect to constrained versus unconstrained edges as well as clamped versus hinged supports at the edges. He concluded that plates with constrained edges exhibited increasing capacity compared to those with unconstrained edges for increasing slenderness and that these plates have a strength reserve which is not taken into account in EN 1993-1-5 [1]. Braun also found that the capacity of plates with clamped plate support compared to hinged supports increased for increasing slenderness. A plated structure in an actual design situation is commonly supported on edges at webs or at adjacent parts which provide rotational and in-plane stiffness. In other cases the plate is part of a continuous structure whereby load-shedding between the various subpanels is possible. It should be noted that the present study of plates under biaxial loads is based on constrained in plane edge displacements and hinged plate supports. Thereby the results are on one hand favourable in terms of the constrained edges but unfavourable since the plate is free to rotate along the support lines.

Valsgård [4] studied sequential loading of biaxially loaded plates for a plate with an aspect ratio of $\alpha = 3$. The research was based on initially loading of the short edges to a certain load level and then he applied loads on the long edges and vica versa. He clarified that non-proportional loading yields a more favourable plate response than proportional loading. A conservative prediction of the post-buckling capacity of biaxially loaded plates therefore has to be based on proportional loading. Valsgård's conclusion was later supported by experimental studies carried out by Stonor et al. [6] which were based on proportional and non-proportional loading of plates with aspect ratios of $\alpha = 4$ and 6. Moreover they clarified that for un-welded plates no difference in maximum capacity was noticed.

The paper by Braun [7] describes the research of Dowling et al. [8] who investigated the influence of the imperfection shape on the capacity of plates by superimposing various buckling modes on the geometry. For a plate with aspect ratio of $\alpha = 3$ under biaxial compression, he determined that the least favourable capacities, in a domain with dominating transverse loads, were found for a single half-wave. In the region with dominating longitudinal load the least favourable loads were obtained with three longitudinal half-waves. The present work, however, contradicts this conclusion and reveals that the least favourable interaction curves are based on imperfection shapes consisting of a larger number of longitudinal half-waves. This conclusion particularly concerns slender plates. Additionally the present research reveals that the plate in some interaction domains no longer is able to maintain the mode of imperfection and experiences a mode transition. In order to develop conservative and reliable interaction curves insight into the various mode transitions in the full interaction domain needs to be established.

Fischer [9] measured the imperfection shapes of fabricated plates and determined that in general plates attain the shape of a single half-wave. The present study shows however, that in order to establish conservative interaction curves it is necessary to include imperfection shapes with shorter half-waves than conventional "quadratic" half-waves. By including short-waved modes thereby is conservative in relation to Fischer's results.

The presented investigations have been performed by the authors and reported in the master thesis of Bondum [10].

1 Imperfection sensitivity analysis

The response of plates subjected to biaxial loads is changing significantly for the different domains in the interaction plane. To outline the difference of the plate behaviour and capacity three representative interaction stress paths for different edge displacement ratios, ζ, are obtained, see Fig. 2. The corresponding interaction stress paths in the biaxial stress domain are illustrated in Fig. 3, which also indicates the interaction curve. The paths are based on an imperfection mode of a single longitudinal half-wave. For $\zeta = 1.0$ the long plate is forced to maintain the imperfection mode throughout the entire loading to collapse as a consequence of the considerable relative transverse edge displacement. For this reason the stress-displacement path for either edge attains a single peak corresponding to the maximum capacity of the plate. For $\zeta = 0.12$ the stress displacement path for the short edge abruptly decreases before it regains stiffness and reaches a second peak. Concurrently the stress-displacement path for the long edge increases considerably subsequent to first peak before it attains a five times larger stress magnitude.

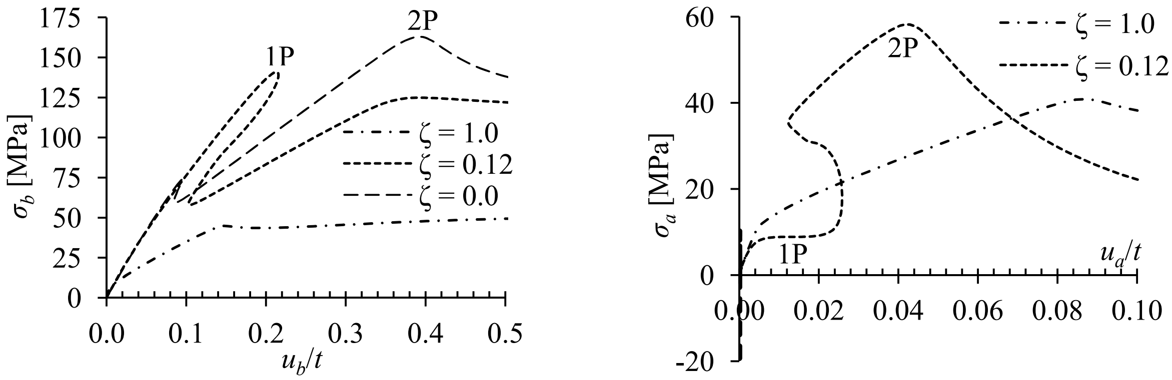

(a) Short edge (b) Long edge

Fig. 2: Stress-displacement paths with imperfection mode A, ($\alpha = 4$, $b/t = 125$)

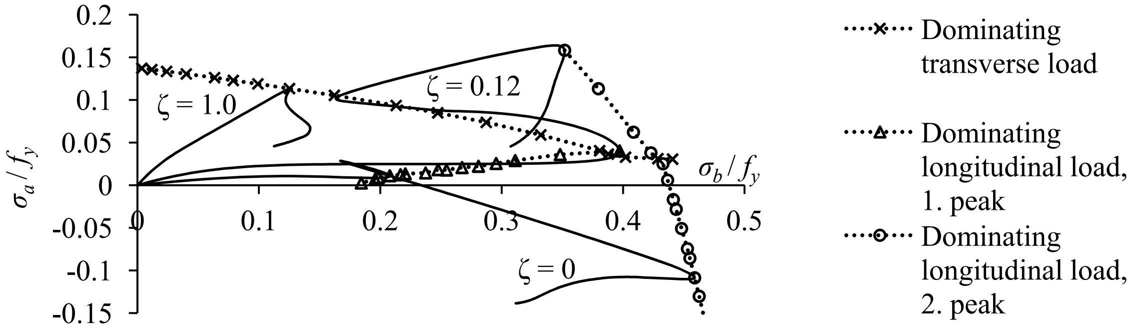

Fig. 3: Interaction curve for buckling with imperfection mode A, ($\alpha = 4$, $b/t = 125$)

The additional peak observed in the Fig. 2 and Fig. 3 is explained by the fact that the plate at a certain low edge displacement ratio experiences a mode transition. At this point the plate is no longer able to maintain the single longitudinal half-wave and is forced to split which results in a shape of the plate consisting of 5 longitudinal half-waves, see Fig. 4. In the following the interaction domain where the transverse compression governs the displacement behaviour with a single longitudinal buckle is defined *dominating transverse compression*, whereas the interaction domain where the longitudinal compression governs the behaviour with multiple buckles is defined *dominating longitudinal compression*. In the presented work the imperfection modes are labelled as imperfection mode A...J corresponding to 1...10 longitudinal half-wave buckles, respectively, without relation to the order of the mode.

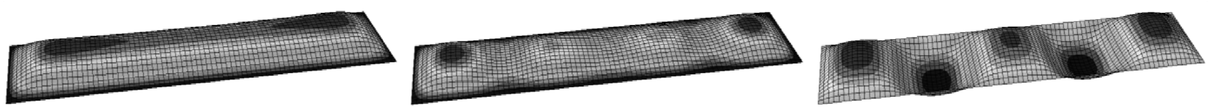

(a) $\zeta = 1.0$ (b) $\zeta = 0.12$, 1. peak (c) $\zeta = 0.12$, 2. peak

Fig. 4: Out-of-plane displacement state in plate at peak ($\alpha = 4$, $b/t = 125$)

The mode transition provides the plate with additional transverse capacity which is constituted by the transverse sections that remain straight. This is the explanation for the jump in maximum transverse stress in Fig. 2(b) and Fig. 3. The mode transition also causes a drop of the longitudinal capacity since the membrane effect in this direction decreases as the shape of the plate consists of an increasing number of buckles. Since the plate for certain modes and regions in the interaction domain experiences mode transitions, it is of interest to investigate the influence of the imperfection shape on the behaviour and capacity for a wide number of modes in order to establish conservative interaction curves in the full interaction domain.

2 Imperfection magnitude according to EN 1993-1-5

For numerical design of steel plates both geometric and structural imperfections should be included. Due to the provisions of EN 1993-1-5, [1], these imperfections can be accounted for by superimposing critical buckling modes on the plate geometry with imperfection magnitude corresponding to the equivalent geometric imperfection

$$i = \min\left(\frac{b}{200}, \frac{a}{200}\right) \tag{1}$$

In order to determine if the approach according to EN 1993-1-5 is conservative, interaction curves are established for a wide number of imperfection modes including the critical which are based on the imperfection magnitude according to the code, see Fig. 5.

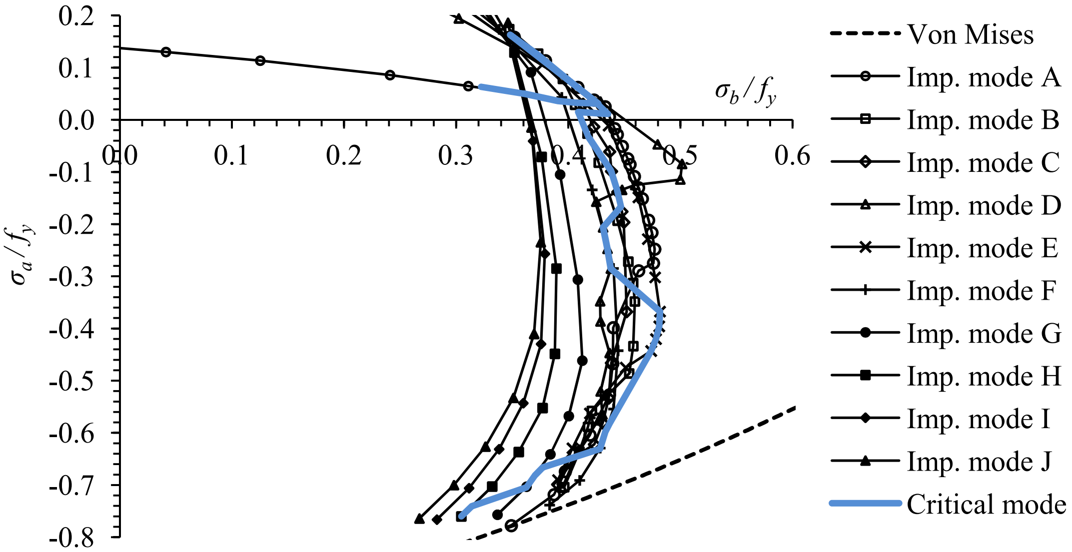

Fig. 5: Interaction curves for imperfection magnitudes according to EN 1993-1-5 ($\alpha = 4$, $b/t = 125$)

The figure illustrates that the interaction curve based on an imperfection shape of the critical mode is far from the most conservative. The longitudinal capacity is seen to decrease for imperfection shapes constituted by larger number of longitudinal half-waves. The imperfection magnitude according to EN 1993-1-5 is, however, very conservative for the short wave length imperfections (multiple imp. buckles). A proposed method to reduce this conservative approach is described in the following.

3 Proposed imperfection magnitude

The imperfection magnitude according to the provisions in EN 1993-1-5 is based on the minimum plate width or length regardless of the shape of the plate. In order to account for the shape of imperfection a proposal of the imperfection magnitude is provided in Bondum [10]. The proposed imperfection magnitude is related to the smallest longitudinal or transverse half-wave length rather than the smallest plate length or width and is formulated by

$$i = \min\left(\frac{b}{n \cdot 200}, \frac{a}{m \cdot 200}\right) \tag{2}$$

Fig. 6 illustrates the imperfection magnitude according to EN 1993-1-5 and the proposed imperfection magnitude for mode A and G.

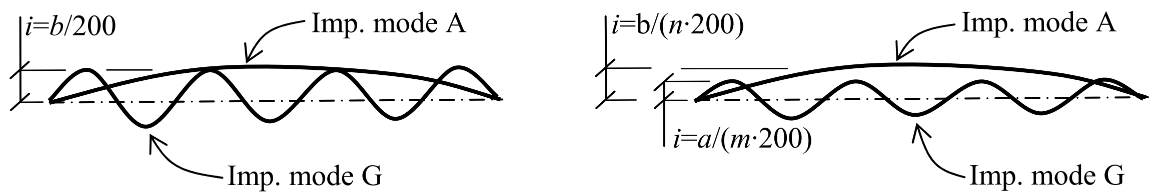

(a) EN 1993-1-5 (b) Novel proposal

Fig. 6: Imperfection magnitude for buckling mode A and G.

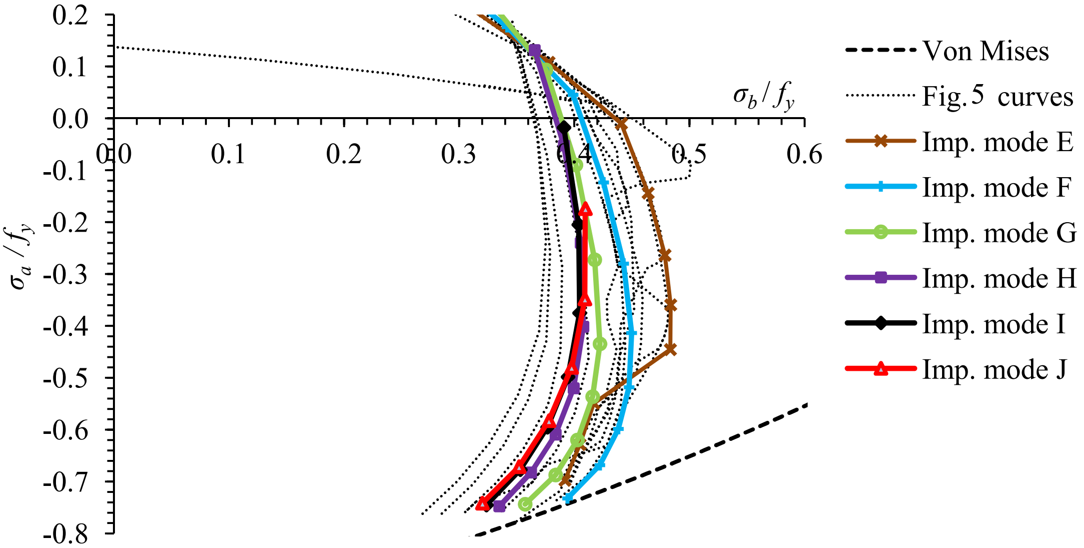

Fig. 7: Interaction curves based on the novel proposal of imperfection magnitudes compared with curves based on imperfection magnitude according to EN 1993-1-5 ($\alpha = 4$, $b/t = 125$).

Interaction curves are established for various imperfection shapes based on the proposed imperfection magnitudes and comparison is made with the curves in Fig. 5. For imperfection shapes constituted by an increasing number of longitudinal half-waves the longitudinal capacity is seen to increase as a consequence of the smaller imperfection magnitude for the higher modes. The figure also shows that the most conservative interaction curve for the proposed imperfection magnitude is constituted by intersecting interaction curves for the various modes. The preceding investigations are used as basis for establishment of conservative interaction curves and corresponding buckling reduction curves in the interaction domain with dominating transverse and longitudinal compression, respectively.

4 Dominating transverse compression

The maximum capacity of the plate is investigated for the interaction domain with dominating transverse compression. In Fig. 8 the interaction stress paths for the plate with an imperfection shape of mode A and B are illustrated. The figure reveals a consistency of the curves which is explained by the fact that the imperfection shape is maintained until collapse. Since the transverse capacity increases for higher number of imperfection buckles, the interaction curve based on the imperfection shape of mode A thereby is the conservative interaction curve in the considered interaction domain.

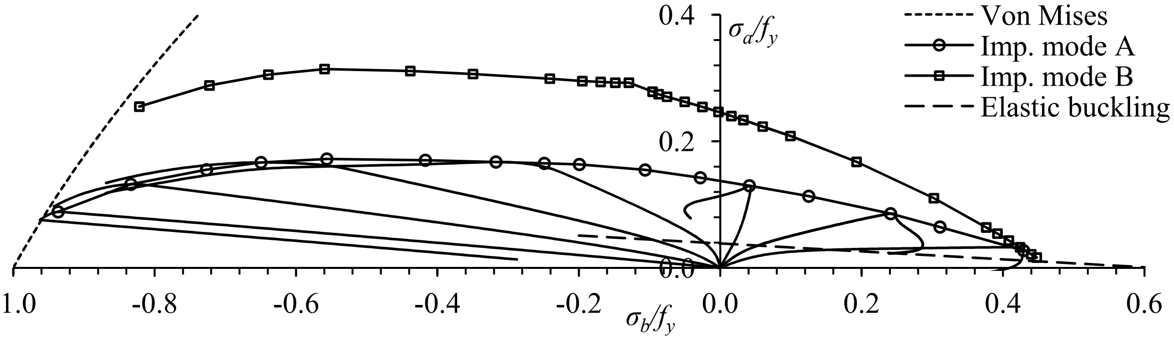

Fig. 8: Conservative interaction curve for dominating transverse compression (α = 4, b/t = 125)

5 Dominating longitudinal compression

In the following the procedure of determining the conservative interaction curve in the interaction domain with dominating longitudinal compression and predominantly transverse tension is described for a plate with $\alpha = 4$ and $b/t = 125$. According to Fig. 7 the conservative interaction curve is constituted by several intersecting interaction curves for various modes.

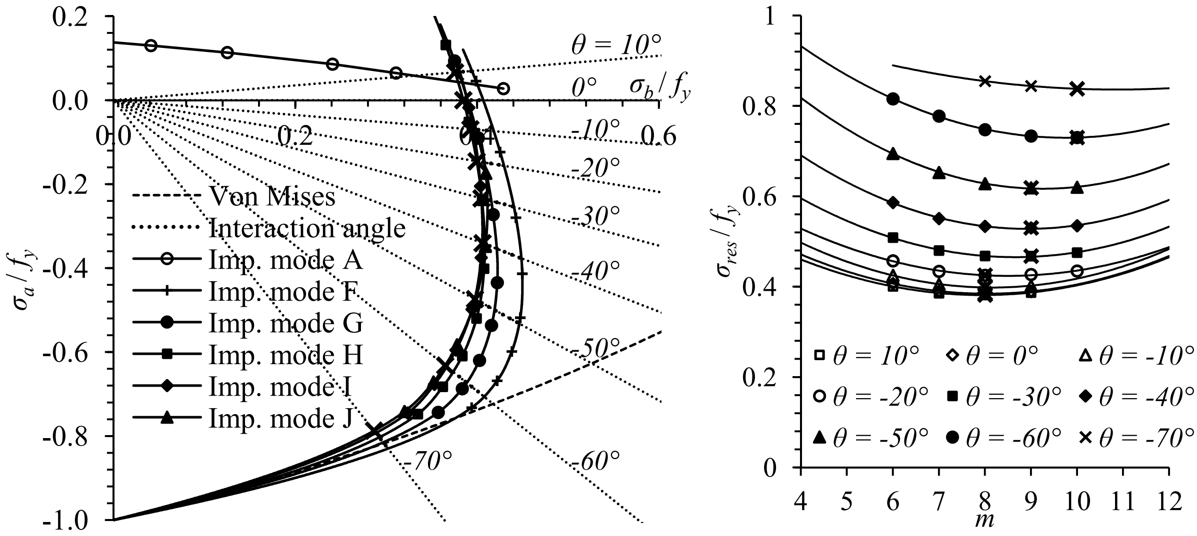

Fig. 9: Conservative interaction curve for dominating longitudinal compression (α = 4, b/t = 125)

A representative number of interaction curves are initially obtained. The representative curves are those which yield responses that are closest to or a part of the conservative interaction curve. For each of the interaction curves interpolated values are calculated and the resulting stress is determined by

$$\sigma_{res} = \sqrt{\sigma_{b,\max}^2 + \sigma_{a,\max}^2} \tag{3}$$

A number of curves with constant interaction stress ratio or interaction angles, θ, are then determined. For the considered plate with slenderness $b/t = 125$ the interaction curves based on mode $G \dots J$ are included, interpolated values and resulting stresses are calculated and the curves with interaction angles $\theta = [10° \dots -70°]$ of $\Delta\theta = 10°$ are used, see Fig. 9. The conservative interaction curve is constituted by the lowest resulting stress obtained for each interaction angle. A convergence test confirms that the obtained lowest resulting stress is the most unfavourable for each interaction angle, see Fig. 9.

6 Conservative interaction curve

To establish the conservative interaction curve in the complete domain a distinctive point of transition from the region with dominating transverse to dominating longitudinal compression needs to be determined. This point corresponds to the transition from buckling mode A to the conservative curve for the higher modes and is defined the *primary transition*. Next the transitions between the higher modes in the range with dominating longitudinal compression are requested. These are defined the *secondary transitions*. For the considered plate geometry the conservative interaction curve in the complete interaction domain is established based on the conservative curves in Section 4 and 5, see Fig. 10, which also illustrates the primary and secondary transitions. The procedure outlined in the preceding is carried out for three additional slenderness values and the corresponding conservative interaction curves with indication of primary and secondary transitions are shown in Fig. 10.

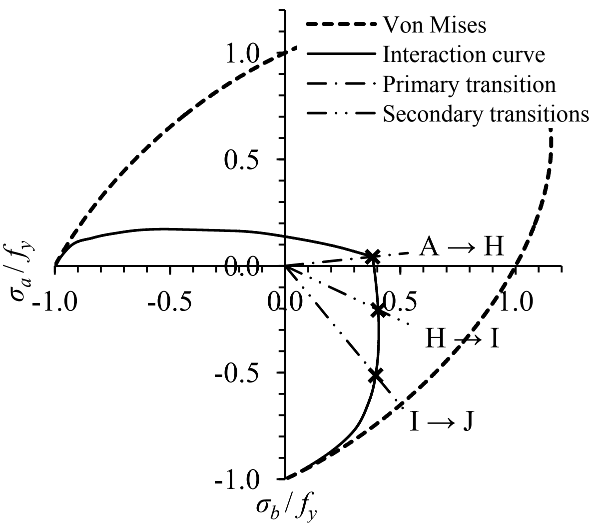

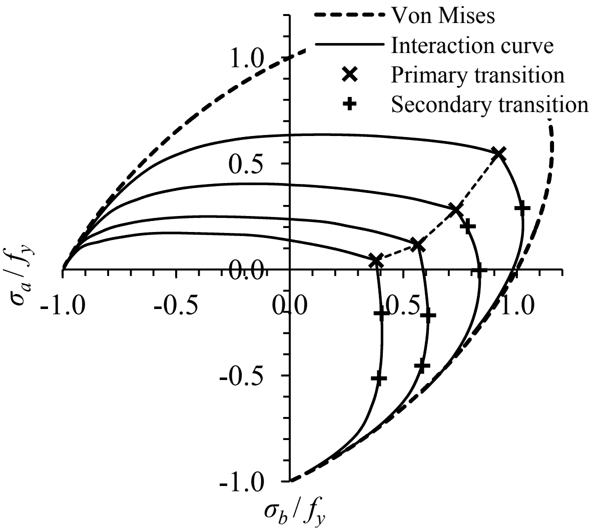

Fig. 10:Conservative interaction curve and primary and secondary transitions

The figure reveals that the primary transitions show a certain tendency in the biaxial plane. The interaction angle for which the primary transition occur, can be formulated by a slenderness relation as:

$$\theta = 748.8 \cdot \left(\frac{b}{t} \right)^{-0.983} \tag{4}$$

Fig. 10 also illustrates that there is no distinctive relation between the locations (and modes) of secondary transitions and the considered slenderness of the plates in the biaxial plane. Therefore an alternative to the use of conservative curves is offered. The curve which yields the least deviating response from the conservative curve is obtained for each slenderness, see Table 1. The alternative interaction curve is noticed to be based on an imperfection shape of a higher mode for increasing plate slenderness.

Table 1: Alternative interaction curves for $\alpha = 4$ and four plate slenderness values

b/t	125	67	40	25
Imp. mode	I	G	E	D

7 Buckling reduction curves

Buckling reduction curves can be determined based on the established conservative interaction curves in Section 6. Initially a number of interaction angles are selected for which the buckling reduction factors are calculated, see Fig. 11(a). A biaxial buckling reduction factor can then be defined as

$$\rho_b = \frac{1}{f_y}\sqrt{\sigma_{b,\max}^2 + \sigma_{a,\max}^2 - \sigma_{b,\max}\sigma_{a,\max}} \tag{5}$$

This can then be used as a reduced stress factor to limit the Von Mises stress by $\sigma_{\mathrm{vm}} \leq \rho_b f_y$. The relation between the buckling reduction factor and relative slenderness i.e. buckling reduction curve for each selected interaction angle is illustrated in Fig. 11(b). The figure reveals consistency of the curves and a formulation for the buckling reduction and relative slenderness that includes the influence of the interaction angle thereby is manageable. The study of Bondum [10] showed that the capacity of the plate for varying aspect ratio is very consistent in the complete interaction domain which implies that it is possible to include the effect of aspect ratio in the formulation.

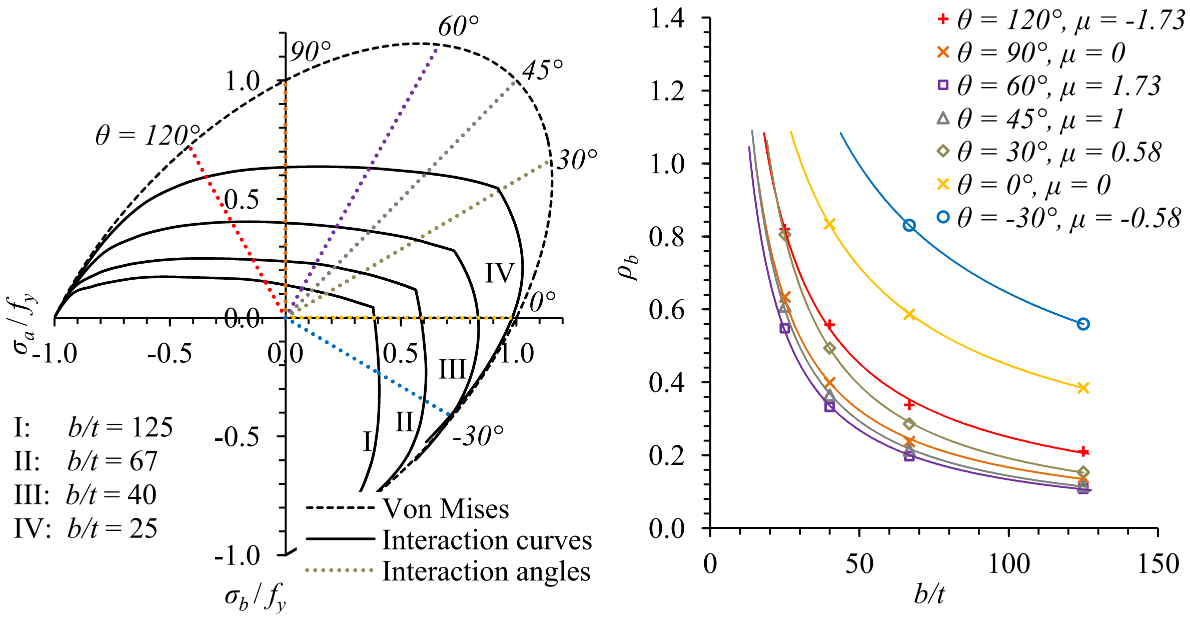

(a) Selected interaction angles (b) Buckling reduction curves

Fig. 11: Interaction angles and corresponding buckling reduction curves ($\alpha = 4$)

8 Conclusions

A detailed investigation of the ultimate capacity of simply supported plates subjected to biaxial loads has been investigated. The full interaction domain of combinations of compressive and tensile loads has been investigated for a variety of imperfections. Following conclusions may be drawn:

1. In parts of the interaction domain non-standard imperfection modes lead to lower ultimate capacity than critical buckling mode imperfections given by the codes.
2. A novel proposal for handling the magnitudes of short-waved imperfections has been proposed. However it has to be calibrated to measured imperfections of real structures.

3. For plate behavior dominated by transverse compression the conservative interaction curves should be based on the imperfection shape of a single longitudinal half-wave.
4. For plate behavior dominated by longitudinal compression the conservative interaction curves should be based on imperfection modes with a large number of half-waves.
5. For each investigated slenderness and interaction angle the capacity of the plate converged towards a certain number of longitudinal half-waves for which the most unfavorable value was obtained.
6. It was found that all the final conservative interaction curves are based on imperfection shapes that do not involve buckling mode transitions.

Furthermore the two investigated plate aspect ratios, $\alpha = 1$ and 2, follow the tendencies observed for the longest plates. Implementation of the effective width concept might be possible since the preceding investigations include both the behaviour and capacity of plates in the complete interaction domain. Finally a potential design proposal should be verified by experiments that reflect the assumptions and parameters.

Acknowledgement

The authors wish to express their gratitude and acknowledge that the investigations of the master project [10] were initiated by co-supervisor Henrik Polk, Senior Project Manager and Head of Section of Major Bridges at COWI A/S, Lyngby, Denmark.

References

[1] EN 1993-1-5. *Eurocode 3 - Design of steel structures - Part 1–5: Plated structural elements,* European Committee for Standardization, Brussels, 2007
[2] ABAQUS CAE, v6.8, Simulia, 2008
[3] EN 1993-1-6, *Eurocode 3 - Design of steel structures - Part 1-6: Strength and stability of shell structures,* European Committee for Standardization, Brussels, 2007
[4] Braun BT. *Stability of steel plates under combined loading*, Dissertation, No. 2010-3, Institute of Structural Design, University of Stuttgart, 2010
[5] Valsgård S. “Numerical design prediction of the capacity of plates in biaxial in-plane compression”, *Computers and Structures*, vol. 12, 729-739, 1980
[6] Stonor RWP, Bradfield CD, Moxham KE. “Tests of Long Plates Under Biaxial Compression”*, J. Construct. Steel Research 24*, 25-56, 1992
[7] Braun BT. “Reduced stress design of plates under biaxial compression”, *Steel Construction 5*, No. 1, 2012
[8] Dowling PS, Harding JE, Slatford JE. “Strength of Ships Plating – Plates in biaxial compression”, *CESLIC Report SP4*, Department of Civil Engineering, Imperial College, London, 1979
[9] Fischer M, Grube R, Rieger H, Wenk P. *Messungen der vorverformungen von beulgefährdeten stahlblechen mit und ohne steifen*, University of Dortmund, 1989
[10] Bondum TH. *Stability Analysis of Biaxially Loaded Steel Plates*, Master Thesis, Department of Civil Engineering, Technical University of Denmark, 2012